

Aus Klinik und Poliklinik für Diagnostische und Interventionelle Radiologie
der Universitätsmedizin der Johannes Gutenberg-Universität Mainz

Dosis und Bildqualität der Photon-Counting HRCT der Lunge

Inauguraldissertation
zur Erlangung des Doktorgrades der
Medizin
der Universitätsmedizin
der Johannes Gutenberg-Universität Mainz

Vorgelegt von

Dr. rer. nat. Dirk Graafen
aus Mainz

Mainz, 2022

Tag der Promotion:

27. Februar 2023

Inhaltsverzeichnis

| | |
|-----------------------------------|----|
| Abkürzungsverzeichnis | I |
| 1 Zusammenfassung | 1 |
| 2 Publikation | 3 |
| 3 Diskussion | 11 |
| 4 Literaturverzeichnis | 13 |
| 5 Tabellarischer Lebenslauf | 16 |

Abkürzungsverzeichnis

| | |
|-------|--|
| ALARA | As Low As Reasonably Achievable |
| BMI | Body Mass Index |
| CT | Computertomographie |
| CTDI | CT-Dosisindex |
| EID | Energie-integrierender Detektor |
| HRCT | High-resolution CT |
| PCD | Photon-Counting Detektor |
| SNR | Signal-Rausch-Verhältnis (signal-to-noise ratio) |

1 Zusammenfassung

Der Einsatz von Photon-Counting Detektoren (PCD) in der Computertomographie (CT) verspricht deutliche Verbesserungen durch hohe räumliche Auflösung, Reduktion des Bildrauschen und inhärente Spektralinformation (1–4). Im Jahr 2021 wurde das erste PCD-CT-Gerät für den klinischen Routinebetrieb zugelassen. Ein solches CT-Gerät wurde im August 2021 in der Klinik für Radiologie der Universitätsmedizin Mainz in Betrieb genommen. Im Gegensatz zu bisherigen CT-Detektoren, bei denen die Röntgenphotonen zunächst in einem Szintillationskristall in optisches Licht umgewandelt werden, entsteht in dem Detektionskristall eines PCD direkt ein elektronisches Signal in Form von Elektron-Loch-Paaren. Durch die direkte Umwandlung in elektronische Impulse beim PCD können einzelne Röntgenphotonen und ihre zugehörige Energie erfasst werden. Im Vergleich dazu werden die Röntgenphotonen und ihre Energie bei konventionellen CT-Detektoren gebündelt erfasst, weshalb diese auch als Energie-integrierende Detektoren (EID) bezeichnet werden.

Die Einführung von CT-Geräten mit Photon-Counting Detektoren (PCD-CT) ermöglicht höhere Auflösungen sowie verbesserte Rauschverhältnisse. Dadurch kann unter anderem die Bildgebung der Lunge relevant verbessert und gleichzeitig die Strahlenexposition minimiert werden (1,5–9). Ziel dieser Arbeit war einen intra-Patienten Vergleich bezüglich Strahlendosis und Bildqualität zwischen der neuen PCD-CT und einer konventionellen EID-CT für die Lungenbildgebung durchzuführen.

In die Untersuchung wurden 32 Patienten eingeschlossen, bei denen sowohl eine hochauflösende CT-Untersuchung der Lunge (high-resolution CT, HRCT) mittels EID-CT als auch mittels PCD-CT verfügbar war. Ausschlusskriterium war ein Unterschied im BMI zwischen den beiden Untersuchungen größer als $2,5 \text{ kg/m}^2$. Zur Bestimmung der Strahlenexposition der CT-Untersuchungen wurde der CT-Dosisindex (CTDI_{vol}) den Dosisberichten entnommen. Eine subjektive Analyse der Bildqualität wurde durch zwei Untersucher unter Verwendung einer 5-Punkte Likert-Skala durchgeführt. Hierfür wurden die Gesamtqualität der Bilder, der Einfluss des Rauschens und Auflösungskriterien des Lungenparenchyms sowie der mediastinalen Strukturen bewertet. Des Weiteren wurden im Rahmen einer quantitativen Bildanalyse das Rauschen in den Bildern sowie das Signal-zu-Rausch-Verhältnis (SNR) im Lungenparenchym, in der Trachea, in der Aorta, im Muskelgewebe und im Hintergrund gemessen.

Der mittlere CTDI_{vol} war bei den Untersuchungen mittels PCD-CT ($0,9 \pm 0,5 \text{ mGy}$) nur halb so groß (Faktor 0,5) wie bei den Untersuchungen mittels EID-CT ($1,8 \pm 0,5 \text{ mGy}$, $p < 0,001$). Die subjektive Bewertung der Bildqualität fiel bei den Bildern der PCD-CT bei beiden Untersuchern

signifikant besser aus ($p < 0,001$). Die quantitative Bildanalyse ergab keine signifikanten Unterschiede bezüglich des Rauschens und des SNR des Lungenparenchyms.

Zusammenfassend konnte in dieser Arbeit gezeigt werden, dass PCD-CT in Kombination mit Zinnfilterung der Röntgenstrahlung zu objektiv stabiler Bildqualität bei halber Strahlenexposition führt, wobei subjektiv in manchen Bewertungskriterien sogar eine Verbesserung der Bildqualität festgestellt wurde. Dadurch konnten Ergebnisse, welche in Studien an PCD-CT Prototypen gewonnen wurden (5–7), im klinischen Routinebetrieb bestätigt werden.

2 Publikation

ORIGINAL ARTICLE

Dose Reduction and Image Quality in Photon-counting Detector High-resolution Computed Tomography of the Chest

Routine Clinical Data

Dirk Graafen, MD, PhD,* Tilman Emrich, MD,†‡
 Moritz C. Halfmann, MD,*‡ Peter Mildenerger, MD,*
 Christoph Düber, MD,* Yang Yang, MD,* Ahmed E. Othman, MD,§
 Jim O' Doherty, PhD,|| Lukas Müller, MD,*
 and Roman Kloeckner, MD*

Purpose: Photon-counting detector computed tomography (PCD-CT) has the potential to significantly improve CT imaging in many ways including, but not limited to, low-dose high-resolution CT (HRCT) of the lung. The aim of this study was to perform an inpatient comparison of the radiation dose and image quality of PCD-CT compared with conventional energy-integrating detector CT (EID-CT).

Methods: A total of 32 consecutive patients with available PCD-CT and EID-CT HRCT scans were included in the final analysis. The CT dose index ($CTDI_{vol}$) was extracted from patient dose reports. Qualitative image analysis comprised the lung parenchyma and mediastinal structures and was assessed by 3 readers using a 5-point Likert scale. Quantitative image analysis included assessment of noise and signal-to-noise ratio in the lung parenchyma, trachea, aorta, muscle, and background.

Results: The mean $CTDI_{vol}$ was 2.0 times higher in the conventional EID-CT scans (1.8 ± 0.5 mGy) compared with PCD-CT (0.9 ± 0.5 mGy, $P < 0.001$). The overall image quality was rated significantly better by all 3 raters ($P < 0.001$) in the PCD-CT relative to the EID-CT. Quantitative analysis showed no significant differences in noise and signal-to-noise ratio in the lung parenchyma between PCD-CT and EID-CT.

Conclusion: Compared with conventional EID-CT scans, PCD-CT demonstrated similar or better objective and subjective image quality at significantly reduced dose levels in an inpatient comparison. These results and their effect on clinical decision-making should be further investigated in prospective studies.

Key Words: high-resolution computed tomography, photon-counting detector, tin filtration, dose reduction

(*J Thorac Imaging* 2022;00:000–000)

From the Departments of *Diagnostic and Interventional Radiology; §Neuroradiology, University Medical Center of the Johannes Gutenberg-University Mainz; ‡German Center for Cardiovascular Research (DZHK), Partner-Site Rhine-Main, Mainz, Germany; †Division of Cardiovascular Imaging, Department of Radiology and Radiological Science, Medical University of South Carolina, Charleston, SC; and ||Siemens Medical Solutions, Malvern, PA.

L.M. and R.K. have contributed equally to this work and are both co-senior authors.

J.O. is a Siemens employee. The remaining authors declare no conflicts of interest.

Correspondence to: Roman Kloeckner, MD, Department of Diagnostic and Interventional Radiology, University Medical Center of the Johannes Gutenberg-University Mainz, Langenbeckst. 1, Mainz 55131, Germany (e-mail: roman.kloeckner@unimedizin-mainz.de).
 Copyright © 2022 Wolters Kluwer Health, Inc. All rights reserved.
 DOI: 10.1097/RTL.0000000000000661

High-resolution computed tomography (HRCT) has become the most important modality for imaging of the lung parenchyma through continuous technical development. However, conventional energy-integrating detector computed tomography (EID-CT) still has several limitations, for example, visualizing fine anatomic lung structures due to limitations of spatial resolution. This limits the diagnostic certainty and therefore directly impacts clinical decision-making.

With its higher spatial resolution and improved noise profile, photon-counting detector computed tomography (PCD-CT) as a novel technique has the potential to considerably improve imaging of the lung parenchyma and surrounding structures, even at a lower radiation dose.^{1,2} Compared with scintillation detectors of EID-CT, photon-counting detectors directly convert x-ray photons into electronic signals allowing separate detection of photons and their associated energies.³ This novel technical development reduces the number of artifacts caused by electronic noise.⁴ Regarding thoracic imaging, the reduction in noise could significantly improve the evaluation of patients with interstitial and alveolar lung disease, in whom even small attenuation changes can be associated with the progression of disease.⁵ Alternatively, PCD-CT has the potential to reduce radiation dose while maintaining image quality, which is especially interesting if using HRCT as a screening tool for lung cancer.¹

In addition, tin filtration has been successfully implemented in chest imaging.⁶ The tin filter is used for spectral shaping as it filters out lower photon energies that do not contribute to final image generation. This allows dose reduction, an increase in the mean energy of the spectrum, and improves image quality characteristics at the interface between the soft tissue and air. This has been shown to have direct benefits in lung and cardiac imaging.⁷

Preliminary patient studies for imaging of the lung parenchyma have shown better objective and subjective image quality of dose-reduced contrast-enhanced chest scans acquired with PCD-CT prototypes compared with dose-matched EID-CT, confirming the promising preclinical results.^{4,8,9} However, little is known about the potential of PCD-CT in terms of dose reduction in daily clinical routine for nonenhanced HRCT.

Therefore, this study aimed to provide a first intra-patient comparison of radiation dose and image quality between a novel PCD-CT combined with spectral shaping by tin filtration, and conventional EID-CT for lung imaging.

METHODS

Study Population

This retrospective study was approved by the local ethics committee of Rhineland-Palatinate, Germany. Informed consent was waived by the ethics committee. Between September 2021 and December 2021, a total of 98 patients underwent HRCT of the lung using the PCD-CT. Thirty-two patients who fulfilled the following criteria were included in the final analysis: (1) age 18 years and above, (2) previous imaging acquired with conventional EID-CT, (3) and no change in the body mass index (BMI) $\geq \pm 2.5$ kg/m² between both scans. A total of 66 patients were excluded for the reasons shown in Figure 1.

Computed Tomography (CT) Protocols and Image Acquisition

All patients were scanned using our institutional standard HRCT protocol with the clinical-approved first-generation dual-source PCD-CT (Naeotom Alpha, Siemens Healthineers, Erlangen, Germany). All patients included in the final analysis also underwent a previous HRCT scan using a conventional single-source EID-CT (Brilliance iCT 256, Philips Healthcare, Eindhoven, the Netherlands) with a clinically established low-dose EID-CT protocol.

While EID-CT was performed at 120 kVp, PCD-CT studies were acquired with 100 kVp and additional tin filtration. Images were reconstructed with identical slice thickness for both scanners. We applied the kernels and strength levels of iterative reconstructions suggested by the different vendors (for the EID-CT: Philips Healthcare; for the PCD-CT: Siemens Healthineers). PCD-CT images were reconstructed using monoenergetic images at 70 keV. Detailed information on the scan protocols, image acquisition, and reconstruction are shown in Table 1.

Radiation Dose Calculation

The CT dose index (CTDI_{vol}) and the dose length product (DLP) of each scan were retrieved from the patient dose report. The effective dose was estimated by multiplying the DLP and the conversion factor for thoracic imaging

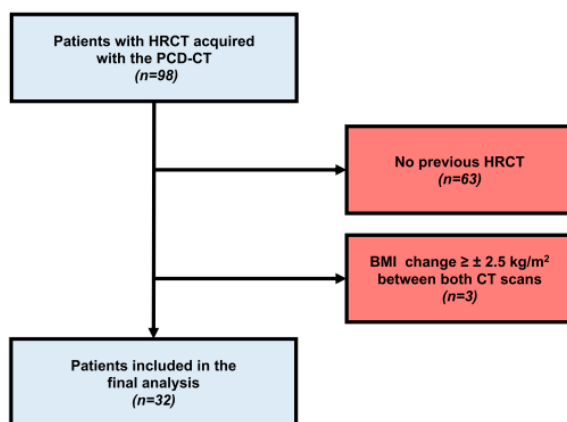


FIGURE 1. Flowchart of study inclusion. [full color online](#)

TABLE 1. Technical Data on CT Protocols and Image Acquisition

| | EID-CT | PDC-CT |
|----------------------------|--------------------|----------------------|
| Manufacturer | Philips Healthcare | Siemens Healthineers |
| Model name | Brilliance iCT 256 | NAEOTOM Alpha |
| Software version | 4.1 | Syngo CT VA40A |
| Single collimation | 0.625 mm | 0.4 mm |
| Total collimation | 80 mm | 57.6 mm |
| Tube voltage | 120 kVp | 100 kVp |
| X-ray filter | — | Tin filter |
| Lung reconstruction | | |
| Iterative reconstruction | iDose (5) | Q4 |
| Convolution kernel | Y-Sharp | BI56 |
| Slice thickness | 1 mm | 1 mm |
| Mediastinal reconstruction | | |
| Iterative reconstruction | iDose (3) | Q2 |
| Convolution kernel | Standard (B) | Br36 |
| Slice thickness | 3 mm | 3 mm |

Both CT scanners use combined longitudinal and angular tube current modulation. Philips: Z-DOM and D-DOM, Siemens: CARE Dose4D.

(0.014).¹⁰ CTDI_{vol} values relate to body CT dosimetry phantoms (PMMA, 32 cm diameter). CTDI_{vol} and DLP were compared in the 3 patient subgroups according to BMI: normal weight ≤ 25 kg/m², overweight 25.0 to 30.0 kg/m², and obese > 30 kg/m².

Qualitative Image Analysis

One board-certified consultant radiologist and 2 residents with 8, 4, and 3 years of experience in thoracic CT imaging, respectively, assessed the subjective image quality in a blinded manner. Image analysis was performed using the in-house picture archiving and communication system (Sectra, Linköping, Sweden). Raters were briefed and trained on how to apply the 5-point Likert scale before the image analysis. A set of 20 patients not included in the study population was read together and a consensus discussion carried out.

For qualitative image analysis of the lung structures, reconstructions with a slice thickness of 1 mm were presented in the in-house standard setting of the lung window (window width 1700 HU, window level -500 HU) with the possibility to change the window settings. The raters assessed the following parameters: overall image quality, noise, artifacts, visually sharp reproduction of the lung parenchyma, resolution of the lung parenchyma including secondary pulmonary lobular structures, lung vessels and fissures, and visually sharp reproduction of the pleuro-mediastinal border and the border between the pleura and the thoracic wall and the resolution between the lung and thoracic wall according to the current version of the European Guidelines on Quality Criteria for Computed Tomography, EUR 16260 (<http://www.drs.dk/guidelines/ct/quality/htmlindex.htm>, last assessed January 31, 2022).

For qualitative image analysis of mediastinal structures, reconstructions with a slice thickness of 3 mm were presented in the in-house standard setting of the mediastinal window (window width 400 HU, window level 60 HU) with the possibility to change the window settings. The raters assessed the following structures: overall image quality, noise, artifacts, and visually sharp reproduction of the trachea, lymph nodes, and esophagus.

The 5-point Likert scale for overall image quality and resolution of the structures had the following categories:

TABLE 2. Baseline Characteristics of the Study Population

| Characteristic | n = 32 |
|--|---------------|
| Median age, years (IQR) | 58 (53-63) |
| Sex, n (%) | |
| Female | 16 (50.0) |
| Male | 16 (50.0) |
| Median body height, cm (IQR) | 171 (166-179) |
| Median body weight, kg (IQR) | 78 (63-86) |
| Mean BMI, kg/m ² (SD) | 25.8 (4.8) |
| Mean BMI change between both scans, kg/m ² (SD) | 0.1 (1.1) |

1 = very poor, 2 = poor, 3 = moderate, 4 = good, 5 = very good. The scale for noise and artifacts had the following categories: 1 = major, 2 = substantial, 3 = moderate, 4 = minor, 5 = none.

Quantitative Image Analysis

An additional radiology resident with 3 years of experience in thoracic CT assessed the objective image quality for all examinations. Regions of interest with an area of 50 to 80 mm² were placed in the vessel-free, non-pathologic lung parenchyma in the upper lobe of both lungs, the supracarinal region of the trachea, the descending aorta, the right autochthonous spinal muscle, and in the background air. Attenuation values and image noise (defined by the standard deviation of the attenuation values) were extracted, and the signal-to-noise ratio (SNR) was calculated by dividing the mean attenuation by the noise of the identical regions of interest.

Statistical Analysis

All statistical analyses and graphic design were performed with R 4.0.3 (A Language and Environment for

Statistical Computing, R Foundation for Statistical Computing, <http://www.R-project.org>; last accessed 31 January 2022). Categorical and binary baseline parameters are reported as absolute numbers and percentages. Ordinal-scaled variables were reported as medians and interquartile ranges. Interval-scaled variables were reported as means and SDs. Distributions between EID-CT and PCD-CT were compared using the 2-sided Wilcoxon rank test. *P*-values <0.05 were considered statistically significant.

RESULTS

Baseline Characteristics

Among the 32 patients included in the analysis, 16 (50.0%) were male. Baseline characteristics of the study population are depicted in Table 2. Median time interval between both scans was 209 days (interquartile ranges 96 to 544 d).

Radiation Dose

Overall, CTDI_{vol} was 2.0 times higher in the conventional EID-CT scans (1.8 ± 0.5 mGy) compared with scans with the PCD-CT (0.9 ± 0.5 mGy, *P* < 0.001) on average. These differences were persistent throughout various BMI classes (Fig. 2). The same tendency was observed for the DLP, which was 2.0 times higher in the conventional EID-CT scans (65.9 ± 17.6 mGy×cm) compared with scans with the PCD-CT (32.5 ± 16.7 mGy×cm, *P* < 0.001) on average. The effective dose was also 2.0 times higher in conventional EID-CT scans (0.92 ± 0.33 mSv) compared with scans with the PCD-CT (0.46 ± 0.27 mSv, *P* < 0.001) on average.

Subjective Image Quality

Regarding quality of the lung images, the overall image quality and visually sharp reproduction of the lung

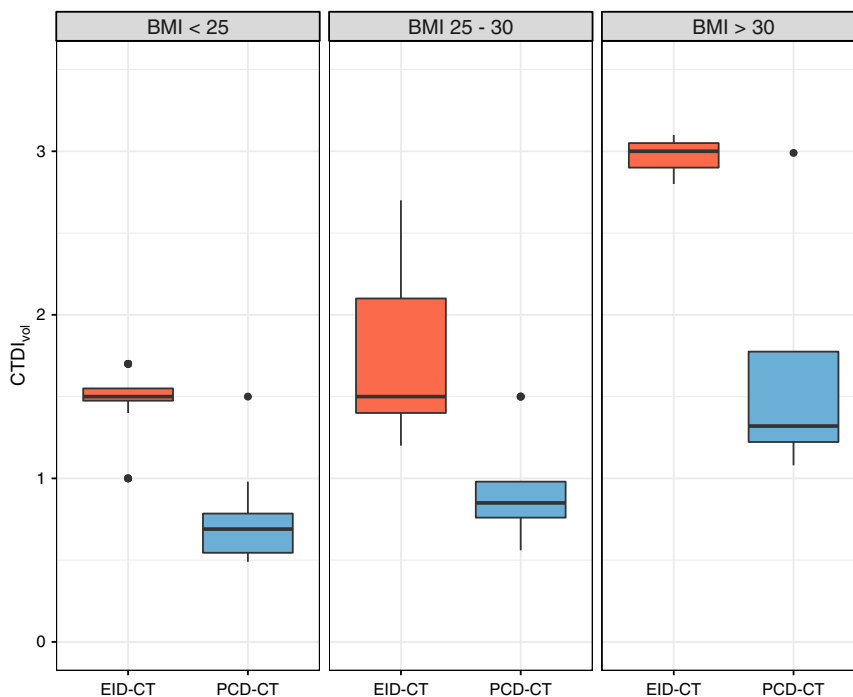


FIGURE 2. CTDI_{vol} between EID-CT and PCD-CT for different intervals of BMI. full color online

parenchyma, lung vessels, pleuromediastinal border, and the border between the lung and the thoracic wall were rated significantly better in PCD-CT scans compared with EID-CT scans (Fig. 3, Table 3). No significant differences were observed for the subjective image noise of the lung parenchyma. A comparison of the evaluation by all 3 raters in consensus and independently is depicted in Table 3. Figure 4 shows an example image for both EID-CT and PCD-CT.

In relation to the subjective quality of mediastinal images, the overall image quality, noise, artifacts, and resolution of the trachea were ranked significantly better in scans acquired with the PCD-CT compared with conventional EID-CT (Fig. 5, Table 4). No significant difference was observed for the resolution of the lymph nodes and the esophagus. A comparison of the evaluation between all three raters is depicted in Table 4.

Objective Image Quality

Concerning objective image quality, no differences were observed for noise and SNR of the lung parenchyma (Table 4). Furthermore, for all mediastinal structures beside the trachea, noise and SNR were significantly better in PCD-CT scans (Table 5).

TABLE 3. Subjective Image Quality of Lung Structures

| | EID-CT | PCD-CT | P |
|--|---------|---------|--------|
| Overall image quality | | | |
| All raters | 4 (3-4) | 4 (4-5) | <0.001 |
| Rater 1 | 4 (4-4) | 5 (4-5) | <0.001 |
| Rater 2 | 3 (3-4) | 4 (4-4) | <0.001 |
| Rater 3 | 4 (3-4) | 4 (4-5) | <0.001 |
| Noise | | | |
| All raters | 3 (3-4) | 3 (3-4) | 0.682 |
| Rater 1 | 4 (4-4) | 4 (3-4) | 0.422 |
| Rater 2 | 3 (3-3) | 3 (3-3) | 0.755 |
| Rater 3 | 3 (3-4) | 4 (3-4) | 0.549 |
| Artifacts | | | |
| All raters | 4 (4-5) | 5 (5-5) | <0.001 |
| Rater 1 | 4 (3-5) | 5 (4-5) | 0.003 |
| Rater 2 | 4 (4-5) | 5 (5-5) | 0.008 |
| Rater 3 | 4 (4-5) | 5 (5-5) | 0.011 |
| Visually sharp reproduction lung parenchyma | | | |
| All raters | 3 (3-4) | 4 (4-5) | <0.001 |
| Rater 1 | 3 (3-4) | 5 (4-5) | <0.001 |
| Rater 2 | 3 (3-4) | 4 (4-4) | <0.001 |
| Rater 3 | 3 (3-4) | 4 (4-5) | <0.001 |
| Visually sharp reproduction lung vessels | | | |
| All raters | 3 (3-4) | 4 (4-5) | <0.001 |
| Rater 1 | 4 (3-4) | 5 (4-5) | <0.001 |
| Rater 2 | 3 (3-3) | 4 (4-4) | <0.001 |
| Rater 3 | 4 (3-4) | 4 (4-5) | <0.001 |
| Visually sharp reproduction pleuromediastinal border | | | |
| All raters | 4 (3-4) | 5 (4-5) | <0.001 |
| Rater 1 | 4 (4-4) | 5 (5-5) | <0.001 |
| Rater 2 | 3 (3-3) | 4 (4-4) | <0.001 |
| Rater 3 | 4 (3-4) | 4 (4-5) | <0.001 |
| Visually sharp reproduction between the lung and thoracic wall | | | |
| All raters | 3 (3-4) | 4 (4-5) | <0.001 |
| Rater 1 | 4 (4-4) | 5 (5-5) | <0.001 |
| Rater 2 | 3 (3-3) | 4 (4-4) | <0.001 |
| Rater 3 | 4 (3-4) | 5 (4-5) | <0.001 |

Values are depicted as median (IQR).

EID-CT indicates conventional energy-integrating CT; PCD-CT, photon-counting CT.

DISCUSSION

This study aimed to investigate the potential benefits of the first-generation dual-source PCD-CT system approved for clinical use with regard to image quality and dose reduction in HRCT scans using an intra-patient comparison.

CTDI_{vol}, DLP, and estimated effective dose were all significantly lower for PCD-CT examinations. These differences remained stable regardless of the patient's BMI. Regarding objective image quality, no significant differences in noise and SNR were observed for the lung parenchyma. However, whereas the EID-CT protocol used a fixed matrix size of 512 resulting in a mean pixel size of 0.8×0.8 mm², an adaptive matrix size algorithm was used at the PCD-CT, which fixes the pixel size for lung reconstructions within a small range of around 0.5×0.5 mm². Therefore, the lung images of the PCD-CT have 60% smaller pixel sizes. Executed on the same CT system, this modification would lead to an equivalent reduction of the SNR, which emphasizes the inherent advantages of the PCD-CT. The SNRs of the mediastinal structures (besides the trachea) were significantly higher in PCD-CT scans. Furthermore, better qualitative imaging ratings were achieved due to the above-mentioned smaller pixel size, in addition to other factors.

PCD-CT has the potential to significantly improve imaging of the lung parenchyma through use of smaller detectors (leading to higher spatial resolution) and the reduction of electronic noise on electronic pulse height analysis. Photon-counting detectors make the indirect photon conversion with a scintillator material into visible photons an unnecessary step.³ So far, only a few preliminary studies have investigated the potential of PCD-CT for imaging of the lung parenchyma with a focus on reconstruction parameters.¹ In a recent study, Si-Mohamed et al¹¹ demonstrated that a matrix of 1024 and a large field-of-view of 300 mm in combination with a small slice thickness of 0.25 mm led to greater conspicuity and sharpness of lung structures with better subjective image quality in scans acquired with a spectral PCD-CT prototype. In this feasibility study a considerable smaller voxel size was used. However, a higher dose (CTDI_{vol} of 1.11 mGy) was necessary even in the low-dose protocol.

Regarding radiation dose and image quality, the results of our study confirm previous in vitro and in vivo results for the potential of PCD-CT in chest imaging.⁴ Through the suppression of electronic noise, PCD-CT may lead to a theoretically better attenuation stability and less image noise at comparable scan parameters. These results were first confirmed on patient scans in 2017, when Symons and colleagues reported up to 16.8% noise reduction and an increase in the lung nodule contrast-to-noise ratio of 21.0%. In their study, PCD-CT dose-reduced contrast-enhanced chest CT yielded better subjective and objective image quality than EID-CT acquired at the same dose levels.

However, to date, a translation of these promising results into the clinical routine is missing. Thus, our results provide an important snapshot of the current capability of PCD-CT when used in clinical routine. Under these circumstances, the substantial dose reduction with acceptable diagnostic image quality may be the most remarkable result of our study. Starting from these benchmarks, future prospective investigations are needed to prove the promising in vitro results for the imaging of specific pathologies such as interstitial lung disease imaging or the characterization of

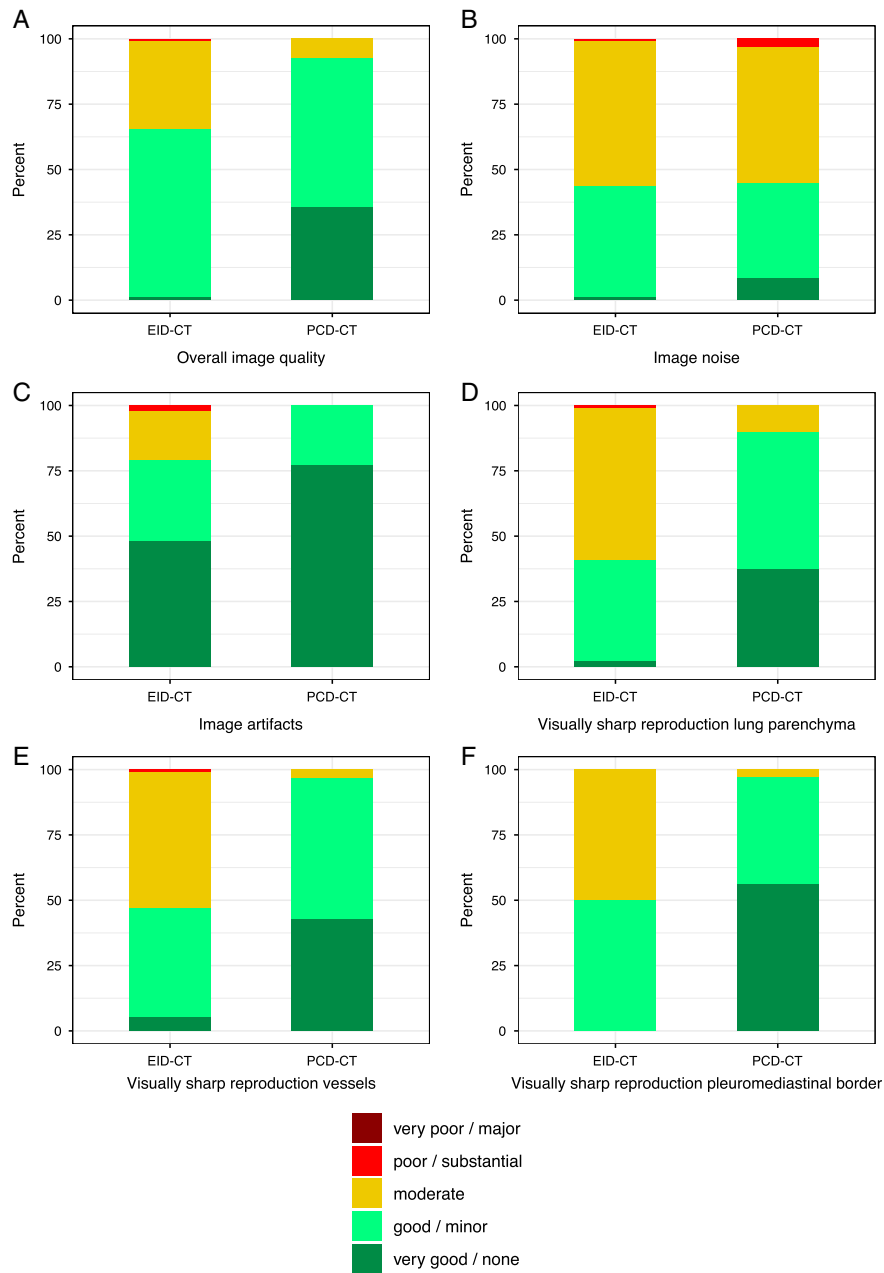


FIGURE 3. Subjective image quality of lung structures. Distribution of the 5-point Likert scale categories for image quality and resolution (very poor, poor, moderate, good, very good) and for noise and artifacts (major, substantial, moderate, minor, none). A Overall image quality, (B) Image noise, (C) Image artifacts, (D) Visually sharp reproduction lung parenchyma, (E) Visually sharp reproduction vessels, (F) Visually sharp reproduction pleuromediastinal border. full color online

lung nodules.^{12,13} The dose reduction may be especially beneficial for use in HRCT for lung cancer screening, in which predominantly healthy persons are examined.

The achieved dose reduction in the PCD-CT is not only caused by the minimum degradation of the PCD from electronic noise but also by the use of a tin filter, which generates a beam hardening of the x-ray spectra. Several studies have investigated the potential of tin filter use in dual-source CT systems for significant dose reduction. Particularly, the application of

ultra-low-dose protocols for lung imaging has been evaluated.^{6,14,15} Haubenreisser et al¹⁶ and Wressnegger et al¹⁷ compared the use of a tin filter for chest CT. In the latter study, an equivalent retrospective design was used comparing a second-generation and a third-generation dual-source CT. They reported a 65% dose reduction while maintaining highly diagnostic image quality. They compared previous CT scans without tin filtration or iterative reconstruction, whereas in our study both lung image reconstructions were performed with the

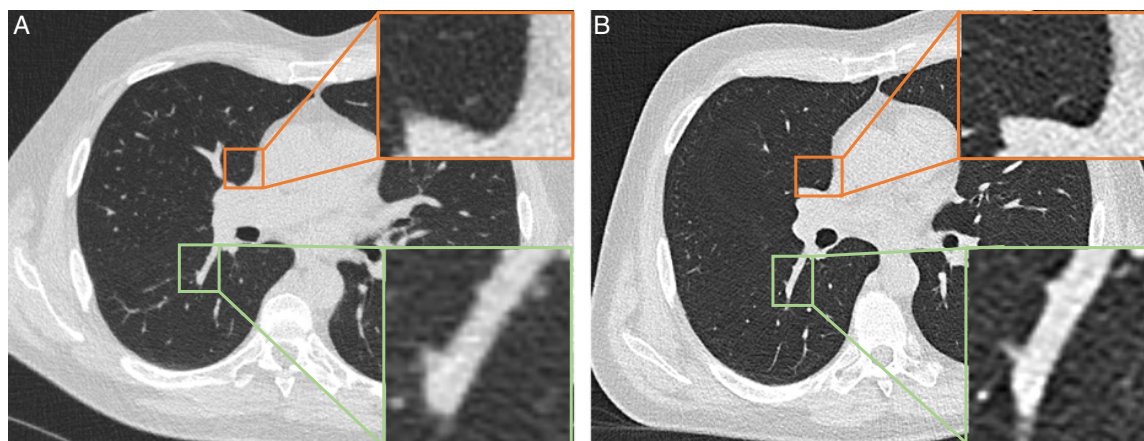


FIGURE 4. Example images for EID-CT (A) and PCD-CT (B) with a focus on visually sharp reproduction of the vessels (green boxes) and the pleuromediastinal border (orange boxes). The time between the acquisition of both scans was 97 days. $CTDI_{vol}$ was 1.5 mGy for the EID-CT scan and 0.8 mGy for the PCD-CT scan. The patient’s BMI was within the category “overweight” and increased ~ 0.9 kg/m² between both scans. [full color online](#)

maximum possible iterative reconstruction level. Furthermore, they reported an effective dose reduction from 3.7 to 1.3 mSv, whereas the dose reduction in our study was on a much lower level (0.92 to 0.46 mSv). Haubenreisser et al¹⁷ reported even a lower effective dose of 0.32 mSv on a third-generation dual-source CT using tin filtration. However, the images were

reconstructed with a slice thickness of 1.5 mm in this study, while we reconstructed the images with a slice thickness of 1.0 mm. Hence, our study compromises the established benefits of tin filtration on the beam side, while using a novel PCD system on the detector side. With this combination, we were able to demonstrate stable image quality at sub-mSv radiation dose levels.

TABLE 4. Subjective Image Quality of Mediastinal Structures

| | EID-CT | PCD-CT | P |
|---|---------|---------|--------|
| Overall image quality | | | |
| All raters | 3 (3-3) | 4 (3-4) | <0.001 |
| Rater 1 | 3 (3-4) | 4 (4-4) | <0.001 |
| Rater 2 | 3 (3-3) | 3 (3-4) | 0.001 |
| Rater 3 | 3 (3-3) | 4 (3-4) | <0.001 |
| Noise | | | |
| All raters | 3 (3-3) | 3 (3-4) | <0.001 |
| Rater 1 | 3 (3-4) | 4 (3-4) | 0.001 |
| Rater 2 | 3 (3-3) | 3 (3-3) | 0.316 |
| Rater 3 | 3 (3-3) | 3 (3-4) | 0.006 |
| Artifacts | | | |
| All raters | 4 (3-5) | 5 (4-5) | <0.001 |
| Rater 1 | 3 (3-4) | 5 (4-5) | <0.001 |
| Rater 2 | 4 (3-5) | 5 (5-5) | <0.001 |
| Rater 3 | 4 (3-5) | 5 (4-5) | 0.001 |
| Visually sharp reproduction trachea | | | |
| All raters | 3 (3-4) | 4 (4-5) | <0.001 |
| Rater 1 | 4 (4-5) | 5 (4-5) | 0.156 |
| Rater 2 | 3 (3-3) | 4 (4-4) | <0.001 |
| Rater 3 | 3 (3-4) | 4 (4-4) | <0.001 |
| Visually sharp reproduction lymph nodes | | | |
| All raters | 3 (3-4) | 3 (3-4) | 0.129 |
| Rater 1 | 4 (4-4) | 4 (4-4) | 0.776 |
| Rater 2 | 3 (3-3) | 3 (3-4) | 0.025 |
| Rater 3 | 3 (3-3) | 3 (3-4) | 0.059 |
| Visually sharp reproduction esophagus | | | |
| All raters | 3 (3-4) | 3 (3-4) | 0.082 |
| Rater 1 | 4 (3-4) | 4 (3-4) | 0.690 |
| Rater 2 | 3 (3-3) | 3 (3-3) | 0.171 |
| Rater 3 | 3 (3-3) | 3 (3-4) | 0.143 |

Values are depicted as median (IQR).
EIC indicates conventional energy-integrating CT; PCCT, photon-counting CT.

Notably, the EID-CT scan protocol has been clinically optimized over the years resulting in a minimum radiation dose for the used slice thickness of 1 mm. At the used EID-CT, slice thickness can be decreased down to 0.67 mm, which would require higher radiation dose values to keep noise and SNR values constant. For the PCD-CT, a default “factory” protocol had been adopted, while no clinical results were available and experience was limited so far. Using equal dose levels in PCD-CT and EID-CT, the latter would presumably have exhibited greater noise and lower qualitative sharpness. In the future, further optimization of scan parameters for the PCD-CT may be achievable resulting in ultra-low-dose high-resolution protocols or low-dose ultra-high-resolution protocols which should be addressed in future studies.

This study is limited by several factors. First and foremost, the study had a retrospective design and was a single-center study with a moderate number of patients. Second, body composition of the patients could have changed between both scans. However, patients with significant BMI changes between both scans were therefore excluded from further analysis. Third, scan protocols for EID-CT and PCD-CT varied with regard to the applied scan parameters, as these were standard settings by the manufacturers. With a total collimation of 57.6 mm and a single collimation of 0.4 mm, we did not use the whole capability of spatial resolution of the PCD-CT, which allows for a single collimation down to 0.2 mm in the ultra-high-resolution (UHR) mode. However, the UHR mode requires higher radiation dose and longer scan times. In our clinical routine, the applied scan parameters enabled an acceptable sharpness of the structures and a good SNR. Furthermore, this allowed for faster scan times leading to less motion artifacts, while dose was within an acceptable range. Nevertheless, the advantages of the UHR mode for high-resolution CT of the chest should be part of future studies. However, although the PCD-CT

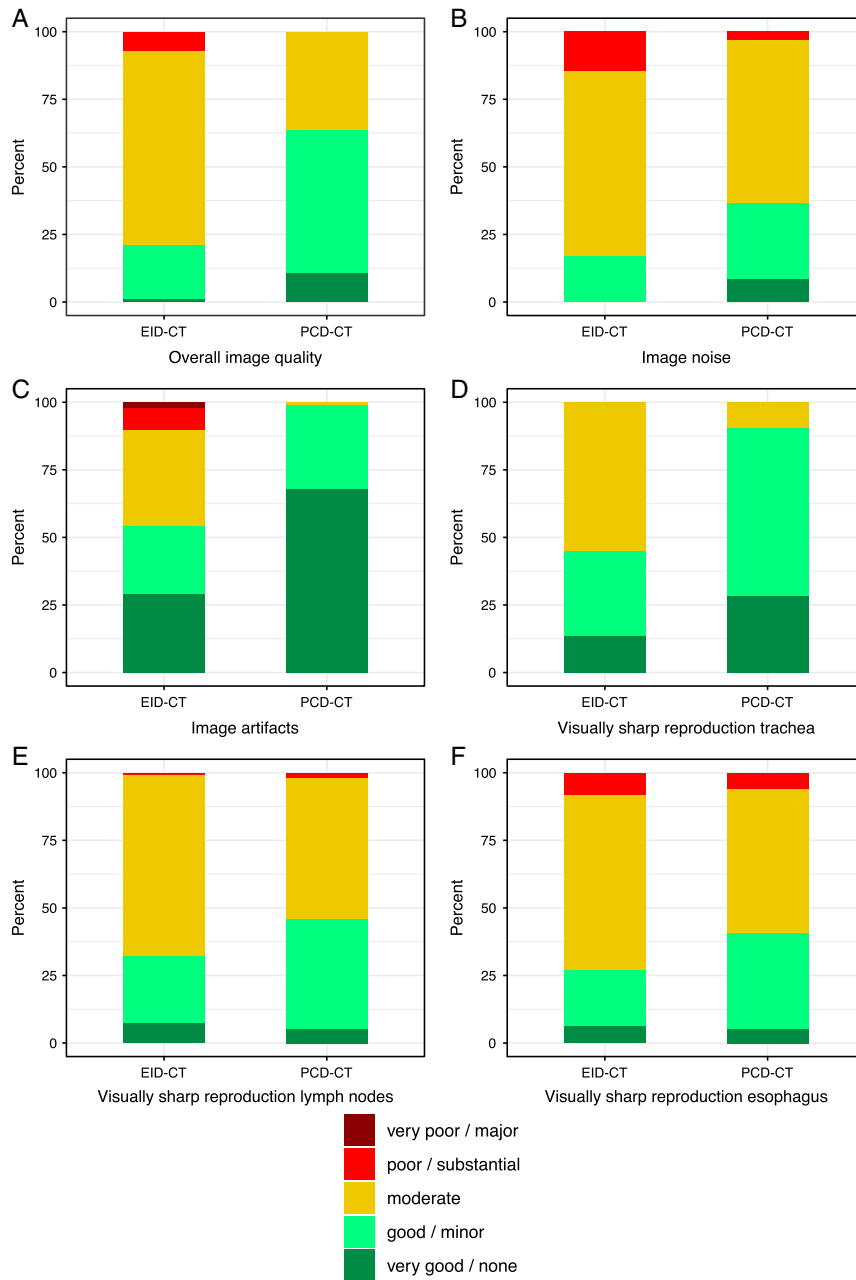


FIGURE 5. Subjective image quality of mediastinal structures. Distribution of the 5-point Likert scale categories for image quality and resolution (very poor, poor, moderate, good, very good) and for noise and artifacts (major, substantial, moderate, minor, none). A, Overall image quality, (B) Image noise, (C) Image artifacts, (D) Visually sharp reproduction trachea, (E) Visually sharp reproduction lymph nodes, (F) Visually sharp reproduction esophagus. [full color online](#)

had a lower kVp potentially leading to higher image noise, significant differences in SNR were observed only for the trachea, whereas the SNR for mediastinal structures was improved in PCD-CT scans. Fourth, we compared the PCD-CT to a more than 10-year-old EID-CT and did not compare our results to the newest state-of-the-art EID-CT scanners. However, this is the current clinical standard in our institution. We believe this could represent a situation that many institutions face in current times when

evaluating whether to purchase a dual-energy, ultra-high-resolution or photon-counting detector system during the renewal process.

In this intra-patient comparison of HRCT scans, PCD-CT with tin filtration led to stable objective and even partially increased subjective image quality at half radiation dose levels compared with conventional EID-CT scans. Thus, this study confirmed preliminary study experiences from PCD-CT prototypes with real-world data, and expands the knowledge about

TABLE 5. Objective Image Quality of Lung and Mediastinal Structures

| Structure | EID-CT | PCD-CT | P |
|-----------------|--------------|---------------|--------|
| Lung parenchyma | | | |
| Attenuation | 894.0 (30.1) | 885.0 (30.5) | 0.235 |
| Noise | 66.9 (19.1) | 70.9 (11.4) | 0.151 |
| SNR | 13.7 (4.1) | 12.5 (2.5) | 0.268 |
| Trachea | | | |
| Attenuation | 971.0 (14.2) | 1002.0 (21.8) | <0.001 |
| Noise | 55.1 (20.8) | 70.7 (11.8) | <0.001 |
| SNR | 19.8 (6.6) | 14.6 (2.7) | <0.001 |
| Aorta | | | |
| Attenuation | 34.5 (10.4) | 38.4 (8.8) | 0.156 |
| Noise | 22.8 (8.0) | 18.4 (3.5) | 0.027 |
| SNR | 1.7 (0.9) | 2.2 (0.7) | 0.027 |
| Muscle | | | |
| Attenuation | 38.0 (10.2) | 47.0 (8.8) | <0.001 |
| Noise | 24.0 (9.0) | 18.8 (4.4) | 0.010 |
| SNR | 1.8 (0.7) | 2.6 (0.8) | <0.001 |
| Background | | | |
| Attenuation | 995.0 (5.8) | 996.0 (7.7) | 0.095 |
| Noise | 18.2 (11.0) | 14.1 (7.4) | 0.016 |
| SNR | 66.1 (23.4) | 80.1 (23.8) | 0.026 |

All numbers are depicted as mean (SD).

improving HRCT application in daily clinical routine by combining spectral shaping with tin filtration and photon-counting detector technology. Effects on clinical decision-making and the applicability of PCD-HRCT on different lung diseases have to be studied in prospective studies.

REFERENCES

- Si-Mohamed SA, Mialhes J, Rodesch P-A, et al. Spectral photon-counting CT technology in chest imaging. *J Clin Med*. 2021;10:5757.
- Willeminck MJ, Persson M, Pourmorteza A, et al. Photon-counting CT: technical principles and clinical prospects. *Radiology*. 2018;289:293–312.
- Taguchi K, Iwanczyk JS. Vision 20/20: single photon counting x-ray detectors in medical imaging. *Med Phys*. 2013;40:100901.
- Symons R, Pourmorteza A, Sandfort V, et al. Feasibility of dose-reduced chest CT with photon-counting detectors: initial results in humans. *Radiology*. 2017;285:980–989.
- Stoel BC, Bode F, Rames A, et al. Quality control in longitudinal studies with computed tomographic densitometry of the lungs. *Proc Am Thorac Soc*. 2008;5:929–933.
- Gordic S, Morsbach F, Schmidt B, et al. Ultralow-dose chest computed tomography for pulmonary nodule detection: first performance evaluation of single energy scanning with spectral shaping. *Invest Radiol*. 2014;49:465–473.
- McQuiston AD, Muscogiuri G, Schoepf UJ, et al. Approaches to ultra-low radiation dose coronary artery calcium scoring based on 3rd generation dual-source CT: a phantom study. *Eur J Radiol*. 2016;85:39–47.
- Symons R, Cork TE, Sahbaee P, et al. Low-dose lung cancer screening with photon-counting CT: a feasibility study. *Phys Med Biol*. 2016;62:202.
- Symons R, Cork T, Folio L, et al. WE-FG-207B-07: feasibility of low dose lung cancer screening with a whole-body photon counting CT: first human results. *Med Phys*. 2016;43:3835.
- Deak PD, Smal Y, Kalender WA. Multisection CT protocols: sex-and age-specific conversion factors used to determine effective dose from dose-length product. *Radiology*. 2010;257:158–166.
- Si-Mohamed S, Boccalini S, Rodesch P-A, et al. Feasibility of lung imaging with a large field-of-view spectral photon-counting CT system. *Diagn Interv Imaging*. 2021;102:305–312.
- Ferda J, Vendiš T, Flohr T, et al. Computed tomography with a full FOV photon-counting detector in a clinical setting, the first experience. *Eur J Radiol*. 2021;137:109614.
- Jungblut L, Blüthgen C, Polacin M, et al. First performance evaluation of an artificial intelligence-based computer-aided detection system for pulmonary nodule evaluation in dual-source photon-counting detector CT at different low-dose levels. *Invest Radiol*. 2022;57:108–114.
- Weis M, Henzler T, Nance JW Jr, et al. Radiation dose comparison between 70 kVp and 100 kVp with spectral beam shaping for non-contrast-enhanced pediatric chest computed tomography: a prospective randomized controlled study. *Invest Radiol*. 2017;52:155–162.
- Martini K, Higashigaito K, Barth BK, et al. Ultralow-dose CT with tin filtration for detection of solid and sub solid pulmonary nodules: a phantom study. *Br J Radiol*. 2015;88:20150389.
- Haubenreisser H, Meyer M, Sudarski S, et al. Unenhanced third-generation dual-source chest CT using a tin filter for spectral shaping at 100 kVp. *Eur J Radiol*. 2015;84:1608–1613.
- Wressnegger A, Prosch H, Moser B, et al. Chest CT in patients after lung transplantation: a retrospective analysis to evaluate impact on image quality and radiation dose using spectral filtration tin-filtered imaging. *PLoS One*. 2020;15:e0228376.

3 Diskussion

Ziel dieser Arbeit war die Vorteile der PCD-CT bei der HRCT der Lunge in einem intra-Patienten Vergleich bezüglich Bildqualität und Dosisreduktion zu untersuchen.

Hierbei konnte erstmalig in der klinischen Routine gezeigt werden, dass die Strahlendosis bei der PCD-CT unabhängig vom BMI der Patienten signifikant reduziert werden konnte und dies sogar bei höherer räumlicher Auflösung. Die gemessenen quantitativen Bildqualitätsparameter des Lungenparenchyms (Rauschen und SNR) zeigten hierbei keinen signifikanten Unterschied. In der subjektiven Bildqualitätsbewertung konnten sogar teils signifikant bessere Ergebnisse erzielt werden. Die erfolgreiche Umsetzung der vielversprechenden Ergebnisse von präklinischen Studien (5,6,8) in die klinische Routine konnte somit eindrucksvoll bestätigt werden.

Im Dezember 2021 veröffentlichte das Bundesamt für Strahlenschutz einen Bericht im Bundesanzeiger (10), in dem die Niedrigdosis-HRCT zur Lungenkrebsfrüherkennung als effektive Methode zur Reduktion der Sterblichkeit bei Raucherinnen und Rauchern dargestellt wird. Dieser Bericht legt die wissenschaftliche Grundlage zur Etablierung eines Lungenkrebsfrüherkennungsprogramms in Deutschland. Da im Rahmen einer Früherkennung vorwiegend gesunde Personen untersucht werden, spielt das Potential der PCD-CT die Untersuchung mit signifikant niedrigeren Dosen durchführen zu können eine besondere Rolle (7). Aber auch bei anderen Indikationen zur Niedrigdosis-HRCT, wie z.B. der Abklärung einer Pneumonie bei Patienten in der Neutropenie, ist die zusätzliche Dosisreduktion im Sinne des ALARA-Prinzips (As Low As Reasonably Achievable) erstrebenswert.

Alternativ kann die PCD-CT in einem ultra-hochauflösenden Modus (ultra-HRCT) verwendet werden, wodurch eine verbesserte Bildqualität erreicht wird (11–14). Dadurch könnten Veränderungen bei alveolären und interstitiellen Lungenerkrankungen besser detektiert werden, z.B. durch Verwendung der Lungendensitometrie (13,15,16). Der klinische Nutzen der ultra-HRCT und besonders inwieweit diese einen relevanten Einfluss auf die Therapieentscheidungen hat oder haben sollte, muss jedoch noch in Studien untersucht werden.

Vorstellbar wäre in Zukunft je nach klinischer Fragestellung zwischen einer ultra-Niedrigdosis-HRCT-Untersuchung und einer Niedrigdosis-ultra-HRCT-Untersuchungen zu wählen. Beide Untersuchungsmethoden können durch die neue PCD-CT in eindrucksvoller Qualität realisiert werden.

In dieser Arbeit konnte das Potential der PCD-CT im Bereich der Dosisreduktion bestätigt werden. Auch partielle Verbesserungen der Bildqualität wurden aufgezeigt. Die PCD-CT bietet zusätzlich noch große Vorteile im Bereich der spektralen CT, bei der die Energieabhängigkeit

der Absorptionskoeffizienten für die Bildgebung ausgenutzt wird. Hierdurch lassen sich unterschiedliche Bestandteile im Bild wie Weichgewebe, Calcium (in Knochen oder Gefäßplaques) oder Kontrastmittel in getrennten Bildern darstellen. Bisherige spektrale CT-Techniken waren methodenbedingt auf zwei Energieinformationen beschränkt (dual-energy CT). Dadurch kann lediglich ein Kontrastmittel aufgelöst werden. Im Bereich der Lungenbildgebung fand die dual-energy CT einerseits im Rahmen der CT-Pulmonalisangiographie Anwendung zur Generierung von pulmonalen Perfusionskarten (17,18). Andererseits können durch die Inhalation von Xenon-Gas Ventilationskarten erzeugt werden (19,20). Die Photon-Counting-Detektoren erlauben mehr als zwei Energieinformationen. Das aktuell zugelassene Gerät bündelt die spektrale Information in vier Energiebereichen. Dadurch können auch mehrere Kontrastmittel in einem CT-Bild voneinander separiert werden (21). Dies könnte zukünftig die zeitgleiche Detektion von Perfusionsbildern und Ventilationsbildern mit einer PCD-CT-Untersuchung der Lunge ermöglichen. Durch die Erfassung von pathologischen Veränderungen sowohl der Lungenventilation als auch der Lungenperfusion könnten Sensitivität und Spezifität der Lungen-CT für viele Lungenerkrankungen verbessert werden könnte.

4 Literaturverzeichnis

1. Willeminck MJ, Persson M, Pourmorteza A, Pelc NJ, Fleischmann D. Photon-counting CT: Technical principles and clinical prospects. *Radiology*. Radiological Society of North America Inc.; 2018. p. 293–312. doi: 10.1148/radiol.2018172656.
2. Flohr T, Petersilka M, Henning A, Ulzheimer S, Ferda J, Schmidt B. Photon-counting CT review. *Physica Medica*. Associazione Italiana di Fisica Medica; 2020. p. 126–136. doi: 10.1016/j.ejmp.2020.10.030.
3. Leng S, Bruesewitz M, Tao S, et al. Photon-counting detector CT: System design and clinical applications of an emerging technology. *Radiographics*. Radiological Society of North America Inc.; 2019;39(3):729–743. doi: 10.1148/rg.2019180115.
4. Wehrse E, Klein L, Rotkopf LT, et al. Photon-counting detectors in computed tomography: from quantum physics to clinical practice. *Der Radiologe*. 2021; doi: 10.1007/s00117-021-00812-8.
5. Ferda J, Vendiš T, Flohr T, et al. Computed tomography with a full FOV photon-counting detector in a clinical setting, the first experience. *European journal of radiology*. *Eur J Radiol*; 2021;137. doi: 10.1016/J.EJRAD.2021.109614.
6. Jungblut L, Blüthgen C, Polacin M, et al. First Performance Evaluation of an Artificial Intelligence-Based Computer-Aided Detection System for Pulmonary Nodule Evaluation in Dual-Source Photon-Counting Detector CT at Different Low-Dose Levels. *Investigative radiology*. *Invest Radiol*; 2022;57(2):108–114. doi: 10.1097/RLI.0000000000000814.
7. Symons R, Cork TE, Sahbaee P, et al. Low Dose Lung Cancer Screening With Photon-Counting CT: A Feasibility Study. *Physics in medicine and biology*. NIH Public Access; 2017;62(1):202. doi: 10.1088/1361-6560/62/1/202.
8. Symons R, Pourmorteza A, Sandfort V, et al. Feasibility of Dose-reduced Chest CT with Photon-counting Detectors: Initial Results in Humans. *Radiology*. *Radiology*; 2017;285(3):980–989. doi: 10.1148/RADIOL.2017162587.
9. Si-Mohamed SA, Miailhes J, Rodesch P-A, et al. Spectral Photon-Counting CT Technology in Chest Imaging. *Journal of clinical medicine*. MDPI; 2021;10(24). doi: 10.3390/jcm10245757.
10. Bundesamt für Strahlenschutz. Lungenkrebsfrüherkennung mittels Niedrigdosis-Computertomographie Wissenschaftliche Bewertung des Bundesamtes für

- Strahlenschutz gemäß § 84 Absatz 3 Strahlenschutzgesetz. urn:nbn:de: 0221-2021082028027. 2021; www.bundesanzeiger.de.
11. Kakinuma R, Moriyama N, Muramatsu Y, et al. Ultra-High-Resolution Computed Tomography of the Lung: Image Quality of a Prototype Scanner. PLoS ONE. Public Library of Science; 2015;10(9):137165. doi: 10.1371/JOURNAL.PONE.0137165.
 12. Miyata T, Yanagawa M, Hata A, et al. Influence of field of view size on image quality: ultra-high-resolution CT vs. conventional high-resolution CT. European Radiology. Springer; 2020;30(6):3324. doi: 10.1007/S00330-020-06704-0.
 13. Xu Y, Yamashiro T, Moriya H, Muramatsu S, Murayama S. Quantitative Emphysema Measurement On Ultra-High-Resolution CT Scans. International Journal of Chronic Obstructive Pulmonary Disease. Dove Press; 2019;14:2283. doi: 10.2147/COPD.S223605.
 14. Hata A, Yanagawa M, Honda O, et al. Effect of Matrix Size on the Image Quality of Ultra-high-resolution CT of the Lung: Comparison of 512 × 512, 1024 × 1024, and 2048 × 2048. Academic Radiology. Elsevier; 2018;25(7):869–876. doi: 10.1016/J.ACRA.2017.11.017.
 15. Mascalchi M, Camiciottoli G, Diciotti S. Lung densitometry: why, how and when. Journal of Thoracic Disease. AME Publications; 2017;9(9):3319. doi: 10.21037/JTD.2017.08.17.
 16. Leutz-Schmidt P, Wielpütz MO, Skornitzke S, et al. Influence of acquisition settings and radiation exposure on CT lung densitometry—An anthropomorphic ex vivo phantom study. PLoS ONE. Public Library of Science; 2020;15(8). doi: 10.1371/JOURNAL.PONE.0237434.
 17. Vlahos I, Jacobsen MC, Godoy MC, Stefanidis K, Layman RR. Dual-energy CT in pulmonary vascular disease. The British journal of radiology. Br J Radiol; 2022;95(1129). doi: 10.1259/BJR.20210699.
 18. de Santis D, Eid M, de Cecco CN, et al. Dual-Energy Computed Tomography in Cardiothoracic Vascular Imaging. Radiologic clinics of North America. Radiol Clin North Am; 2018;56(4):521–534. doi: 10.1016/J.RCL.2018.03.010.
 19. Kong X, Sheng HX, Lu GM, et al. Xenon-enhanced dual-energy CT lung ventilation imaging: techniques and clinical applications. AJR American journal of roentgenology. AJR Am J Roentgenol; 2014;202(2):309–317. doi: 10.2214/AJR.13.11191.

20. Basharat F, Belli M, Kirby M, Tanguay J. Theoretical feasibility of dual-energy radiography for structural and functional imaging of chronic obstructive pulmonary disease. *Medical physics*. *Med Phys*; 2020;47(12):6191–6206. doi: 10.1002/MP.14530.
21. Symons R, Krauss B, Sahbaee P, et al. Photon-counting CT for simultaneous imaging of multiple contrast agents in the abdomen: An in vivo study. *Medical Physics*. 2017;44(10):5120–5127. doi: 10.1002/mp.12301.